

# Sign-switching of dimer correlations in $\text{SrCu}_2(\text{BO}_3)_2$ under high pressure

S. Bettler,\* L. Stoppel, Z. Yan, S. Gvasaliya, and A. Zheludev†  
Laboratory for Solid State Physics, ETH Zürich, 8093 Zürich, Switzerland  
(Dated: May 26, 2022)

Magnetic and vibrational excitations in  $\text{SrCu}_2(\text{BO}_3)_2$  are studied using Raman spectroscopy at hydrostatic pressures up to 34 kbar and temperatures down to 2.6 K. The frequency of a particular optical phonon, the so-called pantograph mode, shows a very strong anomalous temperature dependence below about 40 K. We link the magnitude of the effect to the magnetic exchange energy on the dimer bonds in the Sutherland-Shastry spin lattice in this material. The corresponding dimer spin correlations are quantitatively estimated and found to be strongly pressure dependent. At around  $P_2 \sim 22$  kbar they switch from antiferromagnetic to being predominantly ferromagnetic.

The Shastry-Sutherland model (SSM) is arguably one of the most important constructs in the field of quantum magnetism. It demonstrates that a gapped quantum paramagnet can occur in a well-connected Heisenberg spin Hamiltonian beyond the unique topology of a single dimension. Its key feature is geometric frustration of antiferromagnetic (AF) interactions between AF  $S = 1/2$  dimers arranged on a particular 2-dimensional lattice (Fig. 1a) [1]. For sufficiently strong frustration the *exact* ground state is a product of AF singlets on each dimer bond  $J'$ . For weak frustration one recovers the semi-classical Néel-ordered phase. What happens in-between has been hotly debated [2–20]. The most intriguing intermediate phase proposed is the so-called plaquette state [5, 7, 11]. Dimer singlets are destroyed to be replaced by singlets composed of *four* spins connected via the inter-dimer bonds  $J$ . Translational symmetry is broken and some or all of the dimer spin correlations become *ferromagnetic* (FM).

The only known and much studied experimental realization of the model is  $\text{SrCu}_2(\text{BO}_3)_2$ , where  $S = 1/2$   $\text{Cu}^{2+}$  ions form dimers via Cu-O-Cu superexchange pathways, which are connected through  $(\text{BO}_3)$  units (Fig. 1b) [21]. With a frustration ratio  $J/J' \sim 0.6$  [22] it is reliably in the dimer phase, with a spin gap  $\Delta = 3$  meV [21] in the excitation spectrum. We are incredibly lucky that in this material  $J/J'$  can be continuously tuned by hydrostatic pressure [23]. The frustration ratio increases steadily with pressure, eventually leading to a Néel ordered state above 30 kbar [24]. Moreover, already at  $P_c \sim 18$  kbar the original dimer phase gives way to a new quantum paramagnet, presumed to be the plaquette state [23–27]. Thus, theoretical predictions for exotic phases of the SSM are put to the experimental test.

How can one be sure that the novel phase is indeed plaquette — rather than dimer-based? To date, the only supporting evidence comes from studies of the wave vector dependence of inelastic neutron scattering intensities.[23] Performing such measurements in a bulky cell needed to produce the required pressure for a sufficiently large sample is a formidable task. The resulting data are unavoidably limited and noisy, leaving the interpretation depending on strong assumptions and theoretical modeling [23]. In the present work we use an entirely different approach. We infer the strength of dimer spin correlations in  $\text{SrCu}_2(\text{BO}_3)_2$  from their effect on certain optical phonons, which can be measured using Raman spectroscopy in a diamond-anvil pressure cell. We show that around  $P_c$  these correlations switch from AF to dominantly FM, and thereby independently confirm the destruction of the AF-dimer ground state. Moreover, we obtain a *quantitative* estimate for the dimer bond energy at pressures up to 34 kbar.

The main idea is as follows. As has been established in other dimer systems, the development of pair spin correlations at low temperatures leads to a magnetic contribution to the rigidity of the corresponding bond [28–30]. This, in turn, gives rise to anomalous shifts of certain phonon frequencies at unusually low temperatures set by the magnetic energy scale. In general, each phonon may involve distortions of several magnetic superexchange pathways, making the shifts difficult to associate with any particular spin correlators [30]. For the highly symmetric structure of  $\text{SrCu}_2(\text{BO}_3)_2$  though, the assignment of measured phonons to particular atomic motions is greatly simplified. At  $\hbar\omega \sim 198$   $\text{cm}^{-1}$  ( $=24.5$  meV) there is a specific optical excitation, the so-called pantograph mode, visualized in (Fig. 1b) [31]. It directly modulates the dimer bond length and therefore the intra-dimer coupling con-

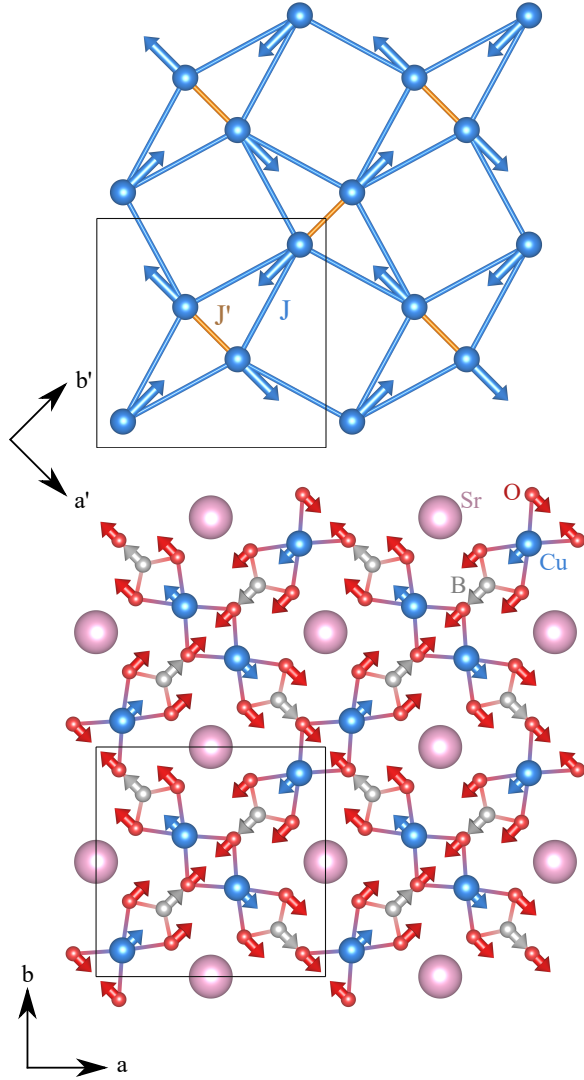


FIG. 1. a) Lattice of orthogonal coupled dimers in  $\text{SrCu}_2(\text{BO}_3)_2$  with intra-dimer interaction  $J'$  and inter-dimer interaction  $J$ . Copper atomic motions of the pantograph mode are indicated as arrows. b) Relative atomic displacements of the pantograph mode in a single layer of  $\text{SrCu}_2(\text{BO}_3)_2$ .

stant  $J'$ . At the same time, it has no first order effect on distances between ions coupled via  $J$ , where its influence is expected to be negligible [31, 32]. Furthermore, its frequency is much larger than the magnetic energy scale, ensuring an adiabatic coupling scenario. To the first approximation, the magnetic shift of the pantograph mode frequency is then sim-

ply proportional to the dimer bond energy  $J'\langle\mathbf{S}_1\mathbf{S}_2\rangle$  averaged over the entire crystal.

Optical phonons, pantograph mode included, as well as purely magnetic excitations, have been extensively studied in  $\text{SrCu}_2(\text{BO}_3)_2$  using Raman spectroscopy at ambient pressure [33–36]. In the present work we perform similar measurements in a 1 mm-culet diamond anvil cell at pressures up to 34 kbar using a Trivista 557 triple-grating spectrometer and a liquid nitrogen cooled CCD detector. The data were collected in a backscattering geometry using a focusing microscope. The incident laser wavelength was 532 nm. The pressure transmitting medium was Argon. The pressure was determined in-situ from ruby fluorescence. The cell environment was a He-flow cryostat with base temperature 2.5 K. All experiments were performed on a  $\sim 0.2 \times 0.1 \times 0.05 \text{ mm}^3$  single crystal sample extracted from cleaving a crystal grown using the floating-zone technique. The incident light was perpendicular to the  $ab$  cleavage plane (see insert in Fig. 2). All spectra shown were measured in the  $\bar{c}(a'b')c$  scattering geometry. An independently measured background from the pressure transmitting medium was subtracted from all spectra.

Optical measurements on  $\text{SrCu}_2(\text{BO}_3)_2$  are extremely challenging due to the narrow band gap of the material, which leads to high absorption [36]. The biggest problem is unwanted heating of the sample by the incident laser beam. To suppress this effect, the data were collected at very low power, as low as 0.05 mW at the lowest temperatures. As a result, typical counting times were as much as 72 h. In all cases it was verified that further reducing the power had no effect on the resulting spectra. A typical low-energy Raman spectrum collected in  $\text{SrCu}_2(\text{BO}_3)_2$  at a pressure of  $P = 2$  kbar and  $T = 2.6$  K is shown in Fig. 2a. The observed frequencies appear fully consistent with previous measurements at ambient pressure [35]. The three visible lowest-energy excitations are magnetic in origin: two triplets and one singlet. All remaining peaks are phonons. The pantograph mode is the peak at around  $198 \text{ cm}^{-1}$ . It was identified by a density functional theory (DFT) ab-initio calculation with the Quantum Espresso software package [37], using the SSSP Accuracy (version 1.1) pseudopotential library [38–44]. The kinetic energy cutoff was 120 Ry and the charge density cutoff 600 Ry. Brillouin zone integration was performed using a  $4 \times 4 \times 4$  k-point grid. For better convergence a Marzari-Vanderbilt

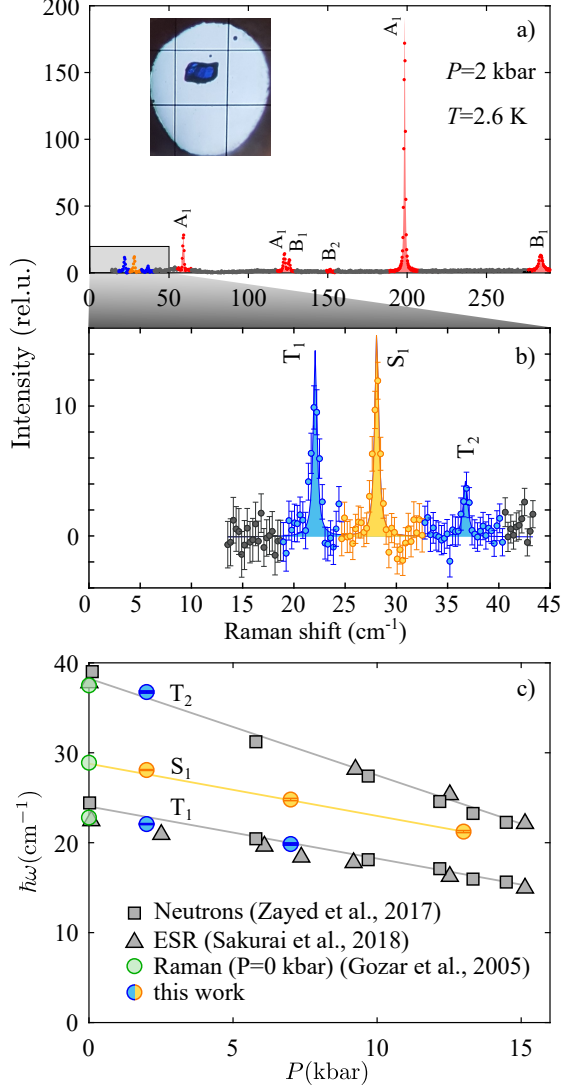


FIG. 2. a) Raman data at  $T \approx 2.6$  K and 2 kbar in  $\bar{c}(a'b')c$  polarization measured with  $\lambda=532$  nm laser. Symmetries of phonons are assigned as in Ref. 35. Inset: picture of the single crystal sample inside the pressure cell along with two ruby spheres used for pressure calibration. b) Blowup of the low-energy portion of a). Triplets  $T_1$  and  $T_2$  and singlet  $S_1$  are assigned according to Ref. 35 c) Comparison of excitation energies of singlet and triplet excitations to published results [23, 27, 35].

cold smearing of 0.01 Ry was applied.

In order to validate the experimental methodology we first checked the behavior of the three *magnetic* excitations. With increasing pressure all three peaks shift to lower energies and progressively weaken. Their measured frequencies are plotted in colored

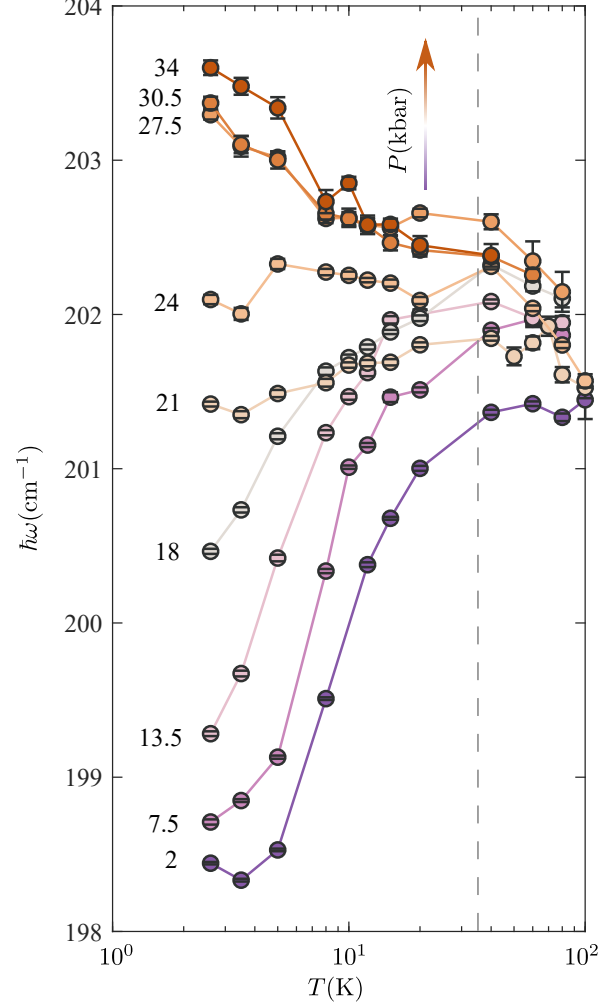


FIG. 3. Measured temperature dependence of the panto-graph mode frequency in  $\text{SrCu}_2(\text{BO}_3)_2$  at different pressures. Note the logarithmic temperature scale. The dashed line is the temperature corresponding to the spin gap energy at ambient pressure.

circles in Fig. 2c. At higher pressures they become undetectably weak or shift outside our measurement window ( $T_1$ ). The observed softening of the triplet modes is fully consistent with previous Electron spin resonance (ESR) [27] and inelastic neutron scattering [23] studies, shown as triangles and squares in the figure. The softening of the singlet mode is a new result, since neither ESR nor neutrons are sensitive to singlet-singlet transitions.

The central result of this work is the observation of an anomalous temperature dependence of the panto-graph mode, as visualized in Fig. 3. Note the loga-

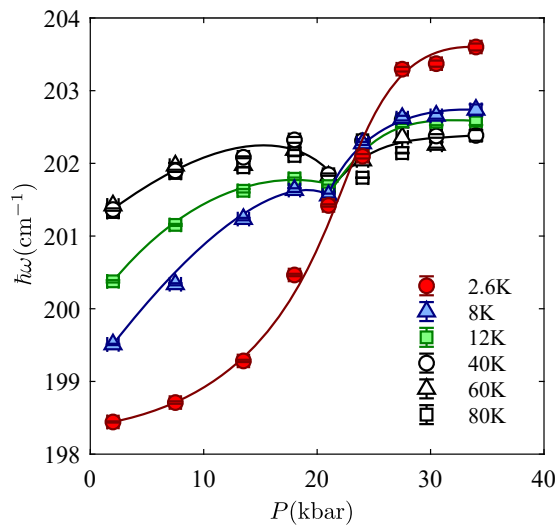


FIG. 4. Measured pressure dependence of the pantograph mode frequency in  $\text{SrCu}_2(\text{BO}_3)_2$  at several different temperatures (symbols). The lines are guides for the eye.

rithmic temperature scale. At all pressures, the pantograph mode undergoes at most a modest hardening upon cooling down to 40 K. This behavior is easily explained by the usual anharmonicities of lattice vibrations. Below this point the mode suddenly becomes strongly  $T$ -dependent. At low applied pressures it *softens* upon cooling to base temperature by as much as 1.5%. At the highest pressures the effect is reversed: in the same low-temperature interval the excitation hardens by as much as 0.5%. Also revealing is the pressure dependence at different temperatures shown in Fig. 4. For  $T \gtrsim 40$  K the pressure dependencies are almost  $T$ -independent. They all show a monotonous hardening with a small but reproducible dip at about 20 kbar. At lower temperatures the situation changes drastically, the frequency showing a steep almost step-like increase.

At temperatures below 40 K, the only remaining relevant energy scale is the magnetic one (of the order of the spin gap  $\Delta$ ). We conclude that the anomalous temperature dependence is due to magnetoelastic coupling and the temperature dependence of spin correlations. The corresponding relative frequency shift of the pantograph mode between 40 K and 2.6 K is plotted against pressure in Fig. 5 (left axis). It remains flat up to about  $P_1 \sim 15$  kbar and then steadily increases up to the highest attainable pressures, switching sign at about  $P_2 \sim 22$  kbar.

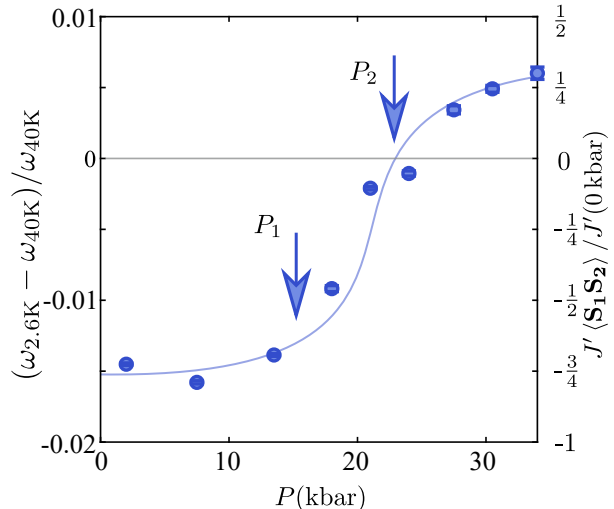


FIG. 5. Pressure dependence of the low-temperature frequency shift of the pantograph mode.  $P_1$  indicates the beginning of the destruction of dimer correlations and  $P_2$  denotes the sign switching of dimer correlations. The solid line is a guide to the eye.

As discussed above, one can view this quantity as a measure of the dimer bond energy. To within a scale factor, Fig. 5 thus represents the pressure dependence of  $J'\langle \mathbf{S}_1 \mathbf{S}_2 \rangle$ . Assuming that  $J'$  is itself only weakly pressure-dependent explains why below  $P_1$  the frequency shift remains roughly constant. Indeed, dimerization in the Shastry-Sutherland model is *exact*, and  $\mathbf{S}_1 \mathbf{S}_2 \equiv -\frac{3}{4}$  regardless of  $J'/J$  [3]. This provides a calibration for the entire plot (Fig. 5, right axis). At  $P_2$  the relative alignment of nearest neighbor spins *switches sign and becomes predominantly ferromagnetic*.

The characteristic pressures found in our experiments closely correspond to those recently observed in high-pressure thermodynamic measurements [24]. According to that study, below  $T_c \sim 2$  K the plaquette state emerges in a discontinuous phase transition just about  $P_1$ . Néel magnetic order sets in at approximately  $P_2$ . The lowest attainable temperature in our experiments is slightly above  $T_c$ . This is consistent with the continuous evolution of  $J'\langle \mathbf{S}_1 \mathbf{S}_2 \rangle$  observed in our case. The sign-switching is thus to be interpreted as a change in the character of dominant *short-range* spin correlations, which are just about to order in a new plaquette configuration at slightly lower temperatures. An important question is whether the pressure-induced changes in the magnetic ground state of  $\text{SrCu}_2(\text{BO}_3)_2$  are driven by

magnetic energy, rather than structural changes due to other causes. We do not observe any unambiguous signs of a pressure-induced structural transition, such as splitting of phonon lines or the appearance of new modes. Nevertheless, the observed dip in the pantograph mode frequency at 20 kbar at temperatures much higher than the magnetic energy scale may be indicative of one.

In summary, our measurements of the pantograph mode in  $\text{SrCu}_2(\text{BO}_3)_2$  provide an indirect but precise quantitative confirmation of a pressure-induced sign switching of nearest-neighbor spin correlations, revealing the demise of dimer-singlets and the emergence of an entirely new ground state where dimer spins are predominantly parallel to one another.

This work was partially supported by the Swiss National Science Foundation, Division 2. We thank D. Blosser (ETHZ) for help with first principles calculations, E. Pomjakushina (PSI) for guidance on the single crystal growth and F. Mila, H. Rønnow and D. Badrtdinov (EPFL) for enlightening discussions.

---

\* sbettler@phys.ethz.ch

† zhelud@ethz.ch; <http://www.neutron.ethz.ch/>

- [1] B. Sriram Shastry and Bill Sutherland, “Exact ground state of a quantum mechanical antiferromagnet,” *Physica B+C* **108**, 1069 – 1070 (1981).
- [2] M. Albrecht and F. Mila, “First-order transition between magnetic order and valence bond order in a 2d frustrated heisenberg model,” *Europhysics Letters (EPL)* **34**, 145–150 (1996).
- [3] Shin Miyahara and Kazuo Ueda, “Exact dimer ground state of the two dimensional Heisenberg spin system  $\text{SrCu}_2(\text{BO}_3)_2$ ,” *Phys. Rev. Lett.* **82**, 3701–3704 (1999).
- [4] Zheng Weihong, C. J. Hamer, and J. Oitmaa, “Series expansions for a Heisenberg antiferromagnetic model for  $\text{SrCu}_2(\text{BO}_3)_2$ ,” *Phys. Rev. B* **60**, 6608–6616 (1999).
- [5] Akihisa Koga and Norio Kawakami, “Quantum phase transitions in the Shastry-Sutherland model for  $\text{SrCu}_2(\text{BO}_3)_2$ ,” *Phys. Rev. Lett.* **84**, 4461–4464 (2000).
- [6] Erwin Müller-Hartmann, Rajiv R. P. Singh, Christian Knetter, and Götz S. Uhrig, “Exact demonstration of magnetization plateaus and first-order dimer-néel phase transitions in a modified Shastry-Sutherland model for  $\text{SrCu}_2(\text{BO}_3)_2$ ,” *Phys. Rev. Lett.* **84**, 1808–1811 (2000).
- [7] Yoshihiro Takushima, Akihisa Koga, and Norio Kawakami, “Competing spin-gap phases in a frustrated quantum spin system in two dimensions,” *Journal of the Physical Society of Japan* **70**, 1369–1374 (2001), <https://doi.org/10.1143/JPSJ.70.1369>.
- [8] David Carpentier and Leon Balents, “Field theory for generalized Shastry-Sutherland models,” *Phys. Rev. B* **65**, 024427 (2001).
- [9] C. H. Chung, J. B. Marston, and Subir Sachdev, “Quantum phases of the Shastry-Sutherland antiferromagnet: Application to  $\text{SrCu}_2(\text{BO}_3)_2$ ,” *Phys. Rev. B* **64**, 134407 (2001).
- [10] Weihong Zheng, J. Oitmaa, and C. J. Hamer, “Phase diagram of the Shastry-Sutherland antiferromagnet,” *Phys. Rev. B* **65**, 014408 (2001).
- [11] Andreas Läuchli, Stefan Wessel, and Manfred Sigrist, “Phase diagram of the quadrumerized Shastry-Sutherland model,” *Phys. Rev. B* **66**, 014401 (2002).
- [12] Mohamad Al Hajj and Jean-Paul Malrieu, “Phase transitions in the Shastry-Sutherland lattice,” *Phys. Rev. B* **72**, 094436 (2005).
- [13] R. Darradi, J. Richter, and D. J. J. Farnell, “Coupled cluster treatment of the Shastry-Sutherland antiferromagnet,” *Phys. Rev. B* **72**, 104425 (2005).
- [14] A. Isacsson and Olav F. Syljuåsen, “Variational treatment of the Shastry-Sutherland antiferromagnet using projected entangled pair states,” *Phys. Rev. E* **74**, 026701 (2006).
- [15] S. Moukouri, “Plaquette ground state of the Shastry-Sutherland model: Density-matrix renormalization-group calculations,” *Phys. Rev. B* **78**, 132405 (2008).
- [16] M. Moliner, I. Rousochatzakis, and F. Mila, “Emergence of one-dimensional physics from the distorted Shastry-Sutherland lattice,” *Phys. Rev. B* **83**, 140414 (2011).
- [17] Philippe Corboz and Frédéric Mila, “Tensor network study of the Shastry-Sutherland model in zero magnetic field,” *Phys. Rev. B* **87**, 115144 (2013).
- [18] David C. Ronquillo and Michael R. Peterson, “Identifying topological order in the Shastry-Sutherland model via entanglement entropy,” *Phys. Rev. B* **90**, 201108 (2014).
- [19] Zhentao Wang and Cristian D. Batista, “Dynamics and instabilities of the Shastry-Sutherland model,” *Phys. Rev. Lett.* **120**, 247201 (2018).
- [20] C. Boos, S.P.G. Crone, I.A. Niesen, P. Corboz, K.P. Schmidt, and F. Mila, “Theory of the intermediate phase of  $\text{SrCu}_2(\text{BO}_3)_2$  under pressure,” arXiv preprint arXiv:1903.07887 (2019).
- [21] H. Kageyama, K. Yoshimura, R. Stern, N. V. Mushnikov, K. Onizuka, M. Kato, K. Kosuge, C. P. Slichter, T. Goto, and Y. Ueda, “Exact dimer ground state and quantized magnetization plateaus in the two-dimensional spin system  $\text{SrCu}_2(\text{BO}_3)_2$ ,” *Phys. Rev. Lett.* **82**, 3168–3171 (1999).
- [22] Christian Knetter and Götz S. Uhrig, “Dynamic structure factor of the two-dimensional Shastry-Sutherland model,” *Phys. Rev. Lett.* **92**, 027204 (2004).

- [23] ME Zayed, Ch Rüegg, AM Läuchli, C Panagopoulos, SS Saxena, M Ellerby, DF McMorro, Th Strässle, S Klotz, G Hamel, *et al.*, “4-spin plaquette singlet state in the shastry–sutherland compound  $\text{SrCu}_2(\text{BO}_3)_2$ ,” *Nature Physics* **13**, 962 (2017).
- [24] Jing Guo, Guangyu Sun, Bowen Zhao, Ling Wang, Wenshan Hong, Vladimir A. Sidorov, Nvsen Ma, Qi Wu, Shiliang Li, Zi Yang Meng, Anders W. Sandvik, and Liling Sun, “Quantum phases of  $\text{Sr}_2\text{Cu}_2(\text{BO}_3)_2$  from high-pressure thermodynamics,” arXiv e-prints, arXiv:1904.09927 (2019).
- [25] S. Haravifard, A. Banerjee, J. C. Lang, G. Srajer, D. M. Silevitch, B. D. Gaulin, H. A. Dabkowska, and T. F. Rosenbaum, “Continuous and discontinuous quantum phase transitions in a model two-dimensional magnet,” *Proceedings of the National Academy of Sciences* **109**, 2286–2289 (2012).
- [26] Takeshi Waki, Koichi Arai, Masashi Takigawa, Yuta Saiga, Yoshiya Uwatoko, Hiroshi Kageyama, and Yutaka Ueda, “A novel ordered phase in  $\text{SrCu}_2(\text{BO}_3)_2$  under high pressure,” *Journal of the Physical Society of Japan* **76**, 073710 (2007), <https://doi.org/10.1143/JPSJ.76.073710>.
- [27] Takahiro Sakurai, Yuki Hirao, Keigo Hiji, Susumu Okubo, Hitoshi Ohta, Yoshiya Uwatoko, Kazutaka Kudo, and Yoji Koike, “Direct observation of the quantum phase transition of  $\text{SrCu}_2(\text{BO}_3)_2$  by high-pressure and terahertz electron spin resonance,” *Journal of the Physical Society of Japan* **87**, 033701 (2018).
- [28] Carsten Raas, Ute Löw, Götz S. Uhrig, and Rainer W. Kühne, “Spin-phonon chains with bond coupling,” *Phys. Rev. B* **65**, 144438 (2002).
- [29] K.-Y. Choi, A. Oosawa, H. Tanaka, and P. Lemmens, “Interplay of triplets and lattice degrees of freedom in the coupled spin dimer system  $\text{KCuCl}_3$ ,” *Phys. Rev. B* **72**, 024451 (2005).
- [30] S. Bettler, G. Simutis, G. Perren, D. Blosser, S. Gvasaliya, and A. Zheludev, “High-pressure raman study of the quantum magnet  $(\text{C}_4\text{H}_{12}\text{N}_2)\text{Cu}_2\text{Cl}_6$ ,” *Phys. Rev. B* **96**, 174431 (2017).
- [31] Guillaume Radtke, Andrés Saúl, Hanna A. Dabkowska, Myron B. Salamon, and Marcelo Jaime, “Magnetic nanopantograph in the  $\text{SrCu}_2(\text{BO}_3)_2$  Shastry–Sutherland lattice,” *Proceedings of the National Academy of Sciences* **112**, 1971–1976 (2015).
- [32] C. Vecchini, O. Adamopoulos, L.C. Chapon, A. Lappas, H. Kageyama, Y. Ueda, and A. Zorko, “Structural distortions in the spin-gap regime of the quantum antiferromagnet  $\text{SrCu}_2(\text{BO}_3)_2$ ,” *Journal of Solid State Chemistry* **182**, 3275 – 3281 (2009).
- [33] P. Lemmens, M. Grove, M. Fischer, G. Güntherodt, Valeri N. Kotov, H. Kageyama, K. Onizuka, and Y. Ueda, “Collective singlet excitations and evolution of raman spectral weights in the 2d spin dimer compound  $\text{SrCu}_2(\text{BO}_3)_2$ ,” *Phys. Rev. Lett.* **85**, 2605–2608 (2000).
- [34] K.-Y. Choi, Yu. G. Pashkevich, K. V. Lamsonova, H. Kageyama, Y. Ueda, and P. Lemmens, “Strong anharmonicity and spin-phonon coupling in the quasi-two-dimensional quantum spin system  $\text{Sr}_{1-x}\text{Ba}_x\text{Cu}_2(\text{BO}_3)_2$ ,” *Phys. Rev. B* **68**, 104418 (2003).
- [35] A. Gozar, B. S. Dennis, H. Kageyama, and G. Blumberg, “Symmetry and light coupling to phononic and collective magnetic excitations in  $\text{SrCu}_2(\text{BO}_3)_2$ ,” *Phys. Rev. B* **72**, 064405 (2005).
- [36] C. C. Homes, S. V. Dordevic, A. Gozar, G. Blumberg, T. Rõõm, D. Hüvonen, U. Nagel, A. D. LaForge, D. N. Basov, and H. Kageyama, “Infrared spectra of the low-dimensional quantum magnet  $\text{SrCu}_2(\text{BO}_3)_2$ : Measurements and *ab initio* calculations,” *Phys. Rev. B* **79**, 125101 (2009).
- [37] Paolo Giannozzi, Stefano Baroni, Nicola Bonini, Matteo Calandra, Roberto Car, Carlo Cavazzoni, Davide Ceresoli, Guido L Chiarotti, Matteo Cococcioni, Ismaila Dabo, Andrea Dal Corso, Stefano de Gironcoli, Stefano Fabris, Guido Fratesi, Ralph Gebauer, Uwe Gerstmann, Christos Gougoussis, Anton Kokalj, Michele Lazzeri, Layla Martinsamos, Nicola Marzari, Francesco Mauri, Riccardo Mazzarello, Stefano Paolini, Alfredo Pasquarello, Lorenzo Paulatto, Carlo Sbraccia, Sandro Scandolo, Gabriele Sciauzero, Ari P Seitsonen, Alexander Smogunov, Paolo Umari, and Renata M Wentzcovitch, “Quantum espresso: a modular and open-source software project for quantum simulations of materials,” *Journal of Physics: Condensed Matter* **21**, 395502 (2009).
- [38] Gianluca Prandini, Antimo Marrazzo, Ivano E. Castelli, Nicolas Mounet, and Nicola Marzari, “Precision and efficiency in solid-state pseudopotential calculations,” *npj Computational Materials* **4**, 72 (2018).
- [39] Kurt Lejaeghere, Gustav Bihlmayer, Torbjörn Björkman, Peter Blaha, Stefan Blügel, Volker Blum, Damien Caliste, Ivano E. Castelli, Stewart J. Clark, Andrea Dal Corso, Stefano de Gironcoli, Thierry Deutsch, John Kay Dewhurst, Igor Di Marco, Claudia Draxl, Marcin Dułak, Olle Eriksson, José A. Flores-Livas, Kevin F. Garrity, Luigi Genovese, Paolo Giannozzi, Matteo Giantomassi, Stefan Goedecker, Xavier Gonze, Oscar Grånäs, E. K. U. Gross, Andris Gulans, François Gygi, D. R. Hamann, Phil J. Hasnip, N. A. W. Holzwarth, Diana Iuşan, Dominik B. Jochym, François Jollet, Daniel Jones, Georg Kresse, Klaus Koepernik, Emine Küçükbenli, Yaroslav O. Kvashnin, Inka L. M. Locht, Sven Lubeck, Martijn Marsman, Nicola Marzari, Ulrike Nitzsche, Lars Nordström, Taisuke Ozaki, Lorenzo Paulatto, Chris J. Pickard, Ward Poelmans, Matt I. J. Probert, Keith Refson, Manuel Richter, Gian-Marco Rignanese, Santanu Saha, Matthias Scheffler, Martin Schlipf, Karlheinz Schwarz, Sangeeta Sharma, Francesca Tavazza,

- Patrik Thunström, Alexandre Tkatchenko, Marc Torrent, David Vanderbilt, Michiel J. van Setten, Veronique Van Speybroeck, John M. Wills, Jonathan R. Yates, Guo-Xu Zhang, and Stefaan Cottenier, “Reproducibility in density functional theory calculations of solids,” *Science* **351** (2016), 10.1126/science.aad3000.
- [40] D. R. Hamann, “Optimized norm-conserving vanderbilt pseudopotentials,” *Phys. Rev. B* **88**, 085117 (2013).
- [41] Martin Schlipf and François Gygi, “Optimization algorithm for the generation of oncv pseudopotentials,” *Computer Physics Communications* **196**, 36 – 44 (2015).
- [42] Gianluca Prandini, Antimo Marrazzo, Ivano E. Castelli, Nicolas Mounet, and Nicola Marzari, “A standard solid state pseudopotentials (sssp) library optimized for precision and efficiency (version 1.1, data download),” (2018).
- [43] Kevin F. Garrity, Joseph W. Bennett, Karin M. Rabe, and David Vanderbilt, “Pseudopotentials for high-throughput dft calculations,” *Computational Materials Science* **81**, 446 – 452 (2014).
- [44] Andrea Dal Corso, “Pseudopotentials periodic table: From h to pu,” *Computational Materials Science* **95**, 337 – 350 (2014).